DALTON

Reaction kinetics and mechanism of formation of $[H_4Co_2Mo_{10}O_{38}]^{6-}$ by peroxomonosulfate oxidation of Co^{II} in the presence of molybdate

Annette L. Nolan, Robert C. Burns and Geoffrey A. Lawrance

Department of Chemistry, The University of Newcastle, Callaghan 2308, New South Wales, Australia

Oxidation of Co^{II} by HSO_5^- to Co^{III} in weakly acidic solution, in the presence of molybdate, resulted in the formation of (primarily) the soluble dicobalt species $[H_4Co_2Mo_{10}O_{38}]^{6-}$. The kinetics of formation of this species was examined at 15–35 °C over the range pH 4.0–5.5 and found to exhibit three separate kinetically observable steps, oxidation of Co^{II} to Co^{III}, followed by a ligand-breakdown reaction and a slow ligand-replacement step which produces the observed product(s). The first stage followed the expanded rate expression $+d[Co^{III}]/dt = k_{ox}[Co^{2+}][HSO_5^-]/[H^+][HMoO_4^-]^3$. A value for k_{ox} of 7.05(4) × 10^{-14} mol^3 dm^{-9} s^{-1} at 25 °C was calculated using reported formation constants describing the speciation of $[MoO_4]^{2-}$, $[Mo_7O_{24}]^{6-}$, and their protonated forms in solution. This rate expression may be accounted for by a mechanism arising from a series of pre-equilibria involving the loss of three $[HMoO_4]^-$ units and a H^+ from a cobalt(II) heteropolymolybdate, most likely $[H_6CoMo_6O_{24}]^{4-}$, which then allows the one-electron oxidation of Co^{2+} to Co^{3+} by HSO_5^- to occur following co-ordination of the latter. In keeping with this proposal, $[NH_4]_4[H_6CoMo_6O_{24}]\cdot 4H_2O$ was crystallized from an acidic (pH 4.5) solution containing $Co^{2+}(aq)$ and molybdate, and its structure determined by X-ray diffraction methods. The heteropolymetalate anion exhibits a standard Anderson structure with six octahedral molybdate edge-sharing units surrounding the central cobalt, and all metal atoms effectively in a common plane. The second observable kinetic step shows no dependences on $[Co^{3+}]$, [oxidant], pH or [molybdate], and is interpreted as a ligand-breakdown reaction, involving loss of an OH• radical from the co-ordinated 'HSO_5^{2-}' (radical) present following the actual one-electron oxidation step. Dimerization is then assumed to occur, followed by slow $[H_4Co_2Mo_{10}O_{38}]^{6-}$ formation stemming from further reaction of the immediate product of the dimerization step, involving loss of co-ordinated SO_4^{2-}.

Despite the extensive investigations of heteropolyoxometalates over decades, studies of the kinetics and mechanisms of their formation have been strictly limited. Recently, we embarked on an investigation of the kinetics of reactions involving the formation of polyoxometalate cage/cluster compounds, with a view to probing their mechanisms of formation. So far, the kinetics of oxidation of manganese(II) by peroxodisulfate ($S_2O_8^{2-}$), peroxomonosulfate (HSO_5^-) and hypochlorous acid (HOCl), and of nickel(II) by $S_2O_8^{2-}$, all in aqueous solution in the presence of molybdate, have been examined, resulting in formation of the species $[MnMo_9O_{32}]^{6-}$ and $[NiMo_9O_{32}]^{6-}$.[1,3] We now report the oxidation of cobalt(II) in the presence of molybdate to give $[H_4Co_2Mo_{10}O_{38}]^{6-}$ as the principal product, using HSO_5^- as oxidant.

Generally, oxidation of Co^{II} in the presence of molybdate gives a mixture of blue-green $[H_6CoMo_6O_{24}]^{3-}$ (the 'monomer') and olive-green $[H_4Co_2Mo_{10}O_{38}]^{6-}$ (the 'dimer'), and care is required to obtain pure samples of each species by the judicious choice of oxidant, pH, temperature and presence (or not) of surface-active catalyst (activated charcoal or Raney nickel).[4] The monomer and dimer are usually produced simultaneously in solution using oxidants such as hydrogen peroxide, bromine and chlorine, where the blue-green monomer species is dominant.[4] When peroxomonosulfate is used as the oxidant, however, the olive-green dimeric species dominates. The product distribution is, however, somewhat dependent on pH, with increasing amounts of the monomer produced at lower pH, which is in agreement with the previously observed instability of $[H_4Co_2Mo_{10}O_{38}]^{6-}$ towards H^+.[5] The dimer has only previously been produced exclusively using hydrogen peroxide as the oxidant with a surface-active catalyst present and, indeed, may be used for the quantitative (spectrophotometric) determination of cobalt.[4] It should be noted that both the monomer and dimer can also be prepared using carbonato- and carbonatoammine-cobalt(III) complexes, without the need for oxidation, with different ligand combinations providing varying yields and selectivities of the two cobalt(III) heteropolymolybdate anions.[6] In view of the dimeric nature of $[H_4Co_2Mo_{10}O_{38}]^{6-}$, it was expected that it would be an excellent candidate for examination of its kinetics of formation, and able to provide further insight into the mechanisms of assembly of polyoxometalate systems. Thus, in the study of the oxidation of manganese(II) by HOCl in the presence of molybdate to give $[MnMo_9O_{32}]^{6-}$, for example, the observed rate law contained concentration terms for both $[MoO_4]^{2-}$ and $[HMoO_4]^-$, indicating for the first time positive evidence for the involvement of these species in the assembly of the polymolybdate cage, rather than preformed isopolymolybdate species such as $[Mo_7O_{24}]^{6-}$.[3] This study will show that two partially built heteropolymolybdate cages can join (dimerize) to produce a large polyoxometalate species containing two heteroatoms, again with the express involvement of monomeric molybdate species. In addition to the kinetic study, we report the crystal structure of $[NH_4]_4[H_6CoMo_6O_{24}]\cdot 4H_2O$, the heteropolyanion which is implicated from the kinetic study as the cobalt(II) species in solution prior to oxidation.

Experimental

Syntheses

Tetraammonium hexahydrogenhexamolybdocobaltate(II) tetrahydrate, $[NH_4]_4[H_6CoMo_6O_{24}]\cdot 4H_2O$. The synthesis was adapted from that reported by La Ginestra *et al.*[7] To a solution containing $[NH_4]_6[Mo_7O_{24}]\cdot 4H_2O$ (24.72 g, 0.020 mol) in water (150 cm^3) was added, drop by drop, a solution (100 cm^3) containing $CoCl_2\cdot 6H_2O$ (4.76 g, 0.020 mol), followed by solid NH_4Cl (2 g) to give a pH of 4.0–4.5. The resulting red solution was covered with a watch-glass and kept in a refrigerator overnight. However, no sign of crystals appeared, as reported

by La Ginestra *et al.*[7] As the solution was allowed to warm slowly to room temperature, however, a pale yellow-orange microcrystalline material formed. These crystals were isolated after 6 d at room temperature. A second crop was isolated after 8 d more and contained very small, thin, pale yellow plates (14.03 g, 60% yield). IR (KBr disc): $\tilde{\nu}_{max}/cm^{-1}$ 929s, 906m (sh), 899m, 876s, 811m (sh) (Mo–O and Co–O stretching), 692m (sh), 639s, 579m, 561m (sh), 475w (Mo–O–Mo and Mo–O–Co stretching). The second crop provided the crystal used in the X-ray study of this compound, as discussed below, and the compound appears to be indefinitely stable in the atmosphere, exhibiting no evidence for loss of water.

Trisodium hexahydrogenhexamolybdocobaltate(III) octahydrate, $Na_3[H_6CoMo_6O_{24}]\cdot 8H_2O$. The synthesis of this compound, for spectroscopic purposes, was essentially as reported by Tsigdinos.[4] UV/VIS (water, pH 4.8): λ_{max}/nm 599 (ε/dm^3 mol^{-1} cm^{-1} 19.7) and 406 (28.7). IR (KBr disc): $\tilde{\nu}_{max}/cm^{-1}$ 948s, 916s (Mo–O and Co–O stretching), 652s, 572s, 539s (sh), 447s (Mo–O–Mo and Mo–O–Co stretching). The crystals lost water of crystallization after several weeks exposure to air to form a green powder, as described by Tsigdinos,[4] possibly $Na_3[H_6CoMo_6O_{24}]\cdot 6H_2O$.

Hexaammonium tetrahydrogendecamolybdodicobaltate(III) heptahydrate, $[NH_4]_6[H_4Co_2Mo_{10}O_{38}]\cdot 7H_2O$. The synthesis of this compound, for spectroscopic purposes, was essentially as reported by Tsigdinos.[4] Under the microscope the black crystals appeared to exist in two different forms as was similarly observed by Evans and Showell.[8] UV/VIS (water, pH 4.8): λ_{max}/nm 599 (ε/dm^3 mol^{-1} cm^{-1} 95.6). IR (KBr disc): $\tilde{\nu}_{max}/cm^{-1}$ 944s, 903s, 862s (sh) (Mo–O and Co–O stretching), 684s, 657s, 629s, 602s, 560s, 526s (Mo–O–Mo and Mo–O–Co stretching).

Physical methods

Electronic spectra were recorded on an Hitachi 150–20 or U-2000 spectrophotometer, infrared spectra as KBr discs using a Bio-Rad FTS-7 Fourier-transform spectrophotometer. Electron spin resonance studies (X-band) were carried out on a Bruker ESP300 spectrometer at a resonance frequency of 9600 MHz employing 100 kHz field modulation. A flat cell, appropriate for aqueous solutions, was employed, and measurements were made at 21 °C.

Kinetic studies

Owing to the speed of the oxidation step and subsequent reaction (see below), both were monitored on an Applied Photophysics SX.17MV stopped-flow spectrophotometer. The data were collected and analysed using an interfaced Archimedes 440/1 computer. The reactions were monitored between 570 and 680 nm at 10 nm intervals. A first-order globalization* procedure involving single-value decomposition of the resulting matrix of absorbance *vs.* time data and subsequent non-linear least-squares fitting was then used to obtain the rate constants.[9] The spectrophotometer was fitted with a thermostatted compartment stable to ±0.1 °C. For the third, slow step in the formation of the product, data were collected at 622 nm on a Hitachi U-2000 spectrophotometer fitted with a thermostatted compartment stable to ±0.1 °C.

Millipore Milli-Q water was used throughout the kinetic studies. Equal volumes of buffered solutions containing Co^{2+}/$[MoO_4]^{2-}$ and HSO_5^- were mixed to obtain the final solutions. Final reaction mixtures contained variable amounts of $CoSO_4\cdot 7H_2O$ (UNIVAR, AR Grade), $Na_2[MoO_4]\cdot 2H_2O$ (UNIVAR, AR Grade) and 'Oxone' ($2KHSO_5\cdot KHSO_4\cdot K_2SO_4$; purity determined as 97.4% using method for $K_2S_2O_8$) (Aldrich)[10] as appropriate, with enough $NaNO_3$ (UNIVAR, AR Grade) to yield a total ionic strength of 1.00 mol dm^{-3}. For the molybdate-dependence study of the first two steps, however, in order to obtain a wide range of Co^{2+}:$[MoO_4]^{2-}$ ratios, solutions were prepared with a total ionic strength of 1.60 mol dm^{-3}. Investigation of the (third) slow kinetically observable step was carried out at higher Co^{2+} and total added $[MoO_4]^{2-}$ concentrations and at an ionic strength of 1.40 mol dm^{-3}, to allow a suitable absorbance change for the spectrophotometer employed. All reaction mixtures were initially prepared using 6 mol dm^{-3} acetic acid–NaOH buffer solutions. The high concentration of buffer was necessary to stabilize the pH due to the acidity of 'Oxone', and the basicity of $[MoO_4]^{2-}$ in solution during polymerization to $[Mo_7O_{24}]^{6-}$. As a result only a slight variation in pH (0.02 unit) was observed over the range of $[MoO_4]^{2-}$ concentrations used at any fixed pH and, similarly, a minor variation in pH (0.04 unit) was observed over the range of HSO_5^- concentrations used.

Crystallography

Crystal data. $[NH_4]_4[H_6CoMo_6O_{24}]\cdot 4H_2O$, $M = 1168.8$, monoclinic, space group $P2_1/c$, $a = 11.364(3)$, $b = 11.130(1)$, $c = 12.008(3)$ Å, $\beta = 109.91(1)°$, $U = 1428.0(5)$ Å^3, $Z = 2$, $D_c = 2.718$ g cm^{-3}, λ(Mo-Kα) = 0.7107 Å, μ(Mo-Kα) = 31.63 cm^{-1}, $F(000) = 1122$, crystal size = 0.034 × 0.11 × 0.14 mm.

Data collection and processing. Reflection data were measured with an Enraf-Nonius CAD-4 diffractometer in θ–2θ scan mode using graphite-monochromated Mo-Kα radiation out to $2\theta_{max} = 50°$. They were corrected for absorption by the method of de Meulenaer and Tompa.[11] A total of 2654 data were collected, giving a data set of 2500 reflections (minimum and maximum transmission factors 0.69 and 0.89) with $I > 3\sigma(I)$ after averaging, with $R_{merge} = 0.012$ for 77 pairs of $hk0$ reflections.

Structure determination. The structure was determined by direct methods using SHELXS 86[12] and the solution refined by Fourier-difference methods using SHELXL 93.[13] However, only four water molecules were located which fits in well with the symmetry of the compound, but differs from the pentahydrated formulation originally proposed by La Ginestra *et al.*[7] on the basis of chemical analysis. Hydrogen atoms were not located, but those attached to the central oxygen atoms of the 'CoO_6' unit at the core of the anion were placed in tetrahedrally located positions with d(O–H) = 0.98 Å. Since the hydrogen atoms could not be located, the differentiation between the N atoms of the NH_4^+ ions and the O atoms of the H_2O molecules proved to be complex. Initially, the precedent used in the case of $[NH_4]_6[Mo_7O_{24}]\cdot 4H_2O$ was followed.[14] In this compound no two NH_4^+ ions were allowed to be closer than 3.7 Å, which is the shortest such distance in $(NH_4)_2O$.[15] In $[NH_4]_6[Mo_7O_{24}]\cdot 4H_2O$ this gave a unique solution, but in the present case still left four possible combinations. The four possible models were refined individually and the final decision made on the basis of $R1$ and $wR2$ (defined below), goodness of fit and, most importantly, parity among the refined thermal parameters of these atoms, that is the least spread in $(U_{11} + U_{22} + U_{33})/3$ values. These were expected to be fairly similar, given the extensive hydrogen-bonded network of the structure, which should result in similar environments for the N atoms of the NH_4^+ ions and the O atoms of the H_2O molecules. Although some doubt must remain that this model is absolutely correct, it should be noted that the resulting average N···O distance of 2.98 Å in the present compound is comparable to that

* 'Globalization' in this context means 'global analysis', and consists of linking common parameters across a series of measurements, *i.e.* the complete analysis of the absorbance *vs.* time data over all wavelengths, resulting in the fitted rate constants.

Table 1 Bond lengths (Å) and angles (°) for $[NH_4]_4[H_6CoMo_6O_{24}]\cdot 4H_2O$ with estimated standard deviations (e.s.d.s) in parentheses

Co–O(123)	2.072(3)	Mo(2)–O(23^I)	1.948(4)
Co–O(112)	2.073(3)	Mo(2)–O(12)	1.955(4)
Co–O(113)	2.074(3)	Mo(2)–O(112)	2.210(3)
Mo(1)–O(1A)	1.707(4)	Mo(2)–O(123^I)	2.249(3)
Mo(1)–O(1B)	1.714(4)	Mo(3)–O(3A)	1.712(4)
Mo(1)–O(13)	1.923(4)	Mo(3)–O(3B)	1.717(4)
Mo(1)–O(12)	1.965(4)	Mo(3)–O(23)	1.924(3)
Mo(1)–O(112)	2.231(3)	Mo(3)–O(13)	1.948(3)
Mo(1)–O(113)	2.250(3)	Mo(3)–O(113)	2.243(3)
Mo(2)–O(2A)	1.711(4)	Mo(3)–O(123)	2.253(3)
Mo(2)–O(2B)	1.711(4)		
O(123)–Co–O(123^I)	180.0	O(112)–Co–O(113^I)	97.47(13)
O(123)–Co–O(112^I)	82.03(13)	O(123)–Co–O(113)	83.15(13)
O(123)–Co–O(112)	97.97(13)	O(112)–Co–O(113)	82.53(13)
O(112^I)–Co–O(112)	180.0	O(113^I)–Co–O(113)	180.0
O(123)–Co–O(113^I)	96.85(13)		
O(1A)–Mo(1)–O(1B)	104.0(2)	O(13)–Mo(1)–O(112)	86.58(14)
O(1A)–Mo(1)–O(13)	97.1(2)	O(12)–Mo(1)–O(112)	71.57(13)
O(1B)–Mo(1)–O(13)	102.0(2)	O(1A)–Mo(1)–O(113)	162.0(2)
O(1A)–Mo(1)–O(12)	101.6(2)	O(1B)–Mo(1)–O(113)	92.0(2)
O(1B)–Mo(1)–O(12)	94.5(2)	O(13)–Mo(1)–O(113)	70.97(13)
O(13)–Mo(1)–O(12)	151.2(2)	O(12)–Mo(1)–O(113)	85.18(14)
O(1A)–Mo(1)–O(112)	91.0(2)	O(112)–Mo(1)–O(113)	75.23(12)
O(1B)–Mo(1)–O(112)	161.5(2)		
O(2A)–Mo(2)–O(2B)	104.5(2)	O(23^I)–Mo(2)–O(112)	84.95(14)
O(2A)–Mo(2)–O(23^I)	101.8(2)	O(12)–Mo(2)–O(112)	72.21(13)
O(2B)–Mo(2)–O(23^I)	96.2(2)	O(2A)–Mo(2)–O(123^I)	89.9(2)
O(2A)–Mo(2)–O(12)	95.2(2)	O(2B)–Mo(2)–O(123^I)	162.8(2)
O(2B)–Mo(2)–O(12)	101.4(2)	O(23^I)–Mo(2)–O(123^I)	71.10(13)
O(23^I)–Mo(2)–O(12)	151.6(2)	O(12)–Mo(2)–O(123^I)	86.50(14)
O(2A)–Mo(2)–O(112)	160.8(2)	O(112)–Mo(2)–O(123^I)	75.17(12)
O(2B)–Mo(2)–O(112)	92.5(2)		
O(3A)–Mo(3)–O(3B)	103.9(2)	O(23)–Mo(3)–O(113)	86.08(14)
O(3A)–Mo(3)–O(23)	102.7(2)	O(13)–Mo(3)–O(113)	70.72(13)
O(3B)–Mo(3)–O(23)	96.9(2)	O(3A)–Mo(3)–O(123)	91.9(2)
O(3A)–Mo(3)–O(13)	95.1(2)	O(3B)–Mo(3)–O(123)	162.3(2)
O(3B)–Mo(3)–O(13)	102.0(2)	O(23)–Mo(3)–O(123)	71.41(13)
O(23)–Mo(3)–O(13)	150.1(2)	O(13)–Mo(3)–O(123)	84.30(14)
O(3A)–Mo(3)–O(113)	161.6(2)	O(113)–Mo(3)–O(123)	75.47(12)
O(3B)–Mo(3)–O(113)	90.8(2)		

Symmetry transformation used to generate equivalent atoms: I $-x + 1, -y, -z$.

of 3.06 Å in $[NH_4]_6[Mo_7O_{24}]\cdot 4H_2O$.[14] There also remains the possibility of positional disorder. Positional and anisotropic thermal parameters for all atoms were refined (on F^2) using full-matrix least squares, and gave an $R1 = 0.0298$ for 2024 reflections $[F_o^2 > 2\sigma(F_o^2)]$ and $wR2 = 0.1013$, where $wR2 = [\Sigma w(F_o^2 - F_c^2)^2/\Sigma(wF_o^4)]^{\frac{1}{2}}$ for all 2500 reflections, with $w = 1/[\sigma^2(F_o^2) + (0.0740P)^2]$, where $P = [\max.(F_o^2,0) + 2(F_c^2)]/3$. The goodness of fit was 0.93. All atomic scattering factors and anomalous dispersion parameters were supplied by SHELXS 86 and SHELXL 93. The structural diagram was produced using ORTEP II,[16] and is shown in Fig. 1, along with the atom numbering scheme. Bond lengths and angles are listed in Table 1.

Atomic coordinates, thermal parameters and bond lengths and angles have been deposited at the Cambridge Crystallographic Data Centre (CCDC). See Instructions for Authors, *J. Chem. Soc., Dalton Trans.*, 1996, Issue 1. Any request to the CCDC for this material should quote the full literature citation and the reference number 186/76.

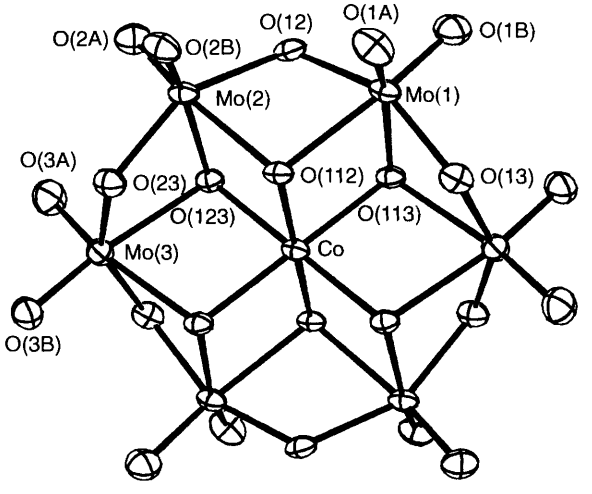

Fig. 1 View of the $[H_6CoMo_6O_{24}]^{4-}$ ion, excluding the hydrogen atoms, which were not crystallographically located

Results and Discussion

Crystal structure of $[NH_4]_4[H_6CoMo_6O_{24}]\cdot 4H_2O$

The structure of $[NH_4]_4[H_6Co^{II}Mo_6O_{24}]\cdot 4H_2O$ consists of ammonium cations, an $[H_6CoMo_6O_{24}]^{4-}$ anion and water molecules of crystallization. The geometry of the anion is based upon the standard Anderson structure with six MoO_6 octahedral edge-sharing units surrounding the central 'CoO_6' octahedron, with all metal atoms essentially in a common

plane. A view of the anion is shown in Fig. 1. In order to balance the cationic charge of the four ammonium ions the six central oxygen atoms surrounding the cobalt are assumed to carry six non-acidic hydrogen atoms, as is typical for low-oxidation-state heteroatoms incorporated into the Anderson structure, *e.g.* $Na_3[H_6CrMo_6O_{24}]\cdot 8H_2O$.[17]

The central cobalt atom is co-ordinated to six oxygen atoms in a slightly distorted octahedral arrangement. There are three crystallographically unique Co–O bonds [2.072(3), 2.073(3) and 2.074(3) Å] with an average of 2.073(3) Å, although the minimum and maximum distances only differ by 1σ. These values may be compared to the Co–O distances found in $[Co(OH_2)_6][SiF_6]$ [2.080(1) Å],[18] the Tutton salt $[NH_4]_2[Co(OH_2)_6][SO_4]_2$ (average 2.092 Å),[18] $Na_2[Co(OH_2)_6][Co(pdta)]_2\cdot 4H_2O$, where pdta = *o*-phenylenedinitrilotetraacetate (average 2.081 Å)[19] and in a range of cobalt(II) acetylacetonate complexes of formulation $Co_n(acac)_{2n}\cdot mH_2O$ (n = 1–4, m = 0–2) (average 2.05 Å).[20] Interestingly, the binary oxide CoO, which has the NaCl structure at room temperature, has a slightly longer Co–O distance (2.125 Å),[21] despite the oxide-like composition of the polymolybdate structure, although none of the oxygen atoms in the present structure is six-co-ordinate as in the CoO structure. In $[H_6CoMo_6O_{24}]^{4-}$ the O–Co–O angles vary from 82.0 to 98.0°, indicating the extent of the angular distortion around the central 'CoO_6' octahedron. Each of the six oxygen atoms co-ordinated to the cobalt atom is, in turn, also co-ordinated to two molybdenum atoms. The molybdenum atoms are also six-co-ordinate, although the distortion away from octahedral symmetry in each case is extensive. Each molybdenum atom is co-ordinated twice to four-co-ordinate oxygen atoms (counting the H atoms attached to these atoms), twice to two-co-ordinate oxygen atoms and twice to one-co-ordinate (*i.e.* terminal) oxygen atoms. The Mo–O bond lengths decrease with decreasing co-ordination number of the oxygen atom, averaging 2.239 Å for four-co-ordination, 1.944 Å for two-co-ordination and 1.715 Å for the terminal oxygen atoms. The six molybdenum atoms form a common plane with the central cobalt atom with a maximum deviation of 0.022 Å out of this plane, and average Co ··· Mo and Mo ··· Mo distances of 3.330(1) and 3.330(3), respectively. All cation–anion and anion–water distances are 2.690 Å or longer (neglecting undetermined hydrogen-atom positions), providing evidence for hydrogen bonding in the structure. The shortest distances are O(W2) ··· O(13) 2.690, O(W1) ··· O(23) 2.702, N(2) ··· O(112) 2.730, and N(2) ··· O(12) 2.743 Å. It should be noted that only four water molecules of crystallization were located, which differs from the pentahydrate formulation originally reported by La Ginestra *et al.*,[7] but based only on elemental analysis. We note in passing that a recent reinvestigation[22] into the synthesis of this compound found only minor amounts of a material which exhibited an infrared spectrum similar to that reported by La Ginestra *et al.*,[7] and concluded that it may not exist. The present study confirms the existence of this species.

Oxidation kinetics

The oxidation of $Co^{2+}(aq)$ by HSO_5^- in the presence of molybdate over the range pH 4.0–5.5 occurs quickly at room temperature (less than *ca.* 10 s for oxidant concentrations from 0.050 to as low as 0.010 mol dm^{-3}), and so a stopped-flow method was employed to monitor this stage of the reaction. Analysis of the data indicated that a fast oxidation step was actually followed by a slightly slower (non-oxidant-dependent) secondary step. The intermediate cobalt(III) species formed after these two reactions has a molar absorption coefficient significantly higher than that of either $[H_4Co_2Mo_{10}O_{38}]^{6-}$ or $[H_6CoMo_6O_{24}]^{3-}$, and was found to decrease with time, indicating further reaction. This latter reaction gave the observed product(s) over a period of *ca.* 3 h, and was monitored using a conventional spectrophotometer. The pH range of the study is limited somewhat by the sensitivity of $[H_4Co_2Mo_{10}O_{38}]^{6-}$ to acid, which is manifested in the final stage of the reaction, as described below. With the exception of the temperature-dependence studies, all the kinetics was monitored at 25.0 °C. The kinetics of the first two steps was monitored between 570 and 680 nm at 10 nm intervals using an automated point-by-point method, followed by global non-linear least-squares fitting, while the final step was monitored at 622 nm, the absorption maximum of the intermediate species produced following the two kinetically faster steps described above.

As indicated above, analysis of the data for the fast kinetic stage showed that it consisted of a rapid oxidation step followed by a slightly slower secondary step, the latter independent of oxidant concentration (see below). Consequently, the data were analysed in terms of two exponentials assuming first-order kinetics for an A ⟶ B ⟶ C type system, and involving two first-order rate constants, k_{ox} and k_2. In general, the rate constant for the slower step (k_2), B ⟶ C, was poorly defined as the band maxima of the intermediates B and C were essentially identical within experimental error (622 nm). However, the molar absorption coefficients of B and C were found to vary relative to each other with pH, and therefore $[MoO_4^{2-}]$, and also to some extent with $[HSO_5^-]$ (at high pH). As a result, the rate constant for the second reaction was better defined under conditions whereby the molar absorption coefficient of C was lower than that of B. The relative variation in the molar absorption coefficient of B and C was used to advantage in establishing the oxidant dependences of k_{ox} and k_2. Initial investigations involved conditions under which the molar absorption coefficients of B and C were almost identical, and the rate constants k_{ox} and k_2 similar in magnitude. This therefore allowed the use of a single exponential for the analysis of the rate data for the formation of Co^{III}. Once this dependence was established the experimental conditions were varied so that the molar absorption coefficients of B and C were different and, assuming that the same dependence for k_{ox} applied under these conditions, the latter could be fixed and the dependence of k_2 on $[HSO_5^-]$ investigated. Values for the rate constants k_{ox} and k_2 under various conditions are given in Tables 2–5. In these tables the reported errors are those resulting from the spread of values obtained from at least four separate determinations. However, in view of the difficulties in determining an accurate value of k_2 in many cases, the errors in this rate constant are likely to be considerably greater than quoted (see below). The final slow step, C ⟶ D, follows these first two rapid reactions, and is also defined by a first-order rate constant (k_3). Data for this step, including the product distribution with pH, are given in Table 6.

Step 1, the oxidation. The kinetic data were analysed in terms of the first-order rate law governed by k_{ox}, a pseudo-first-order rate constant which subsumes dependences on $[HSO_5^-]$ and, as will be shown below, an inverse dependence on $[H^+]$ and an inverse third-order dependence on $[HMoO_4^-]$. The rate constant k_{ox} shows a first-order dependence on $[HSO_5^-]$ at pH 4.22 (established using a single exponential for analysis of the rate data, as described above). Thus, a plot of $\log k_{ox}$ against $\log [HSO_5^-]$ gives a straight line with a slope of 0.96(6) (R^2 = 0.9985), giving the expanded rate expression (1) where k'_{ox} is

$$+d[Co^{III}]/dt = k'_{ox}[Co^{2+}][HSO_5^-] \qquad (1)$$

27.4(4) $dm^3\ mol^{-1}\ s^{-1}$ at 25 °C. This value is an average over each of the HSO_5^- concentrations employed. The rate expression is consistent with HSO_5^- participating as a one-electron oxidant, a consequence of the one-electron oxidation of Co^{II} to Co^{III} despite being formally a two-electron oxidant.

In order to determine the potential dependences of the rate on $[H^+]$ and $[MoO_4^{2-}]$, the variations of k_{ox} with both pH and

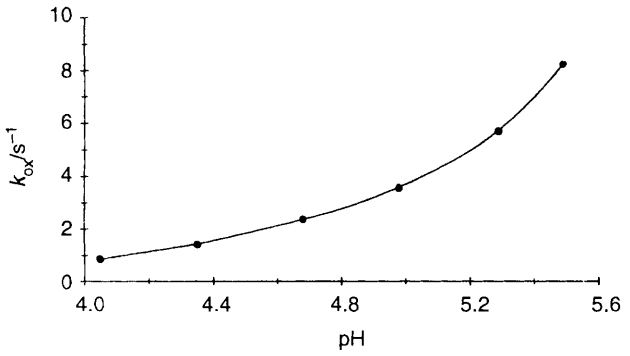

Fig. 2 Dependence of k_{ox} on pH. $[Co^{2+}] = 0.0025$, $[HSO_5^-] = 0.030$, $[MoO_4^{2-}]_T = 0.0625$, $I = 1.00$ mol dm^{-3}, 25.0 °C

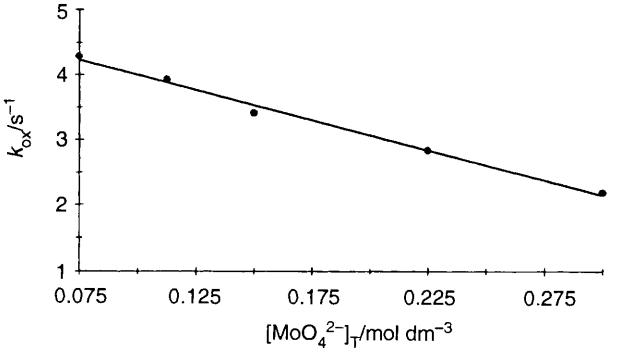

Fig. 3 Dependence of k_{ox} on total added molybdate. $[Co^{2+}] = 0.0015$, $[HSO_5^-] = 0.018$, pH 5.20, $I = 1.60$ mol dm^{-3}, 25.0 °C

Table 2 Observed rate constants, k_{ox} and k_2, for oxidation of cobalt(II) by peroxomonosulfate in the presence of molybdate: oxidant dependence ($[Co^{2+}] = 0.0025$ mol dm^{-3}, $[MoO_4^{2-}]_T = 0.0625$ mol dm^{-3}, pH 4.22 ± 0.02 or 5.13 ± 0.03, $I = 1.00$ mol dm^{-3}, 25.0 °C)

$[HSO_5^-]$/mol dm^{-3}	pH	k_{ox}/s^{-1}	k_2/s^{-1}
0.010	4.22	0.28(1)	—[a]
	5.13	—	—
0.020	4.22	0.56(1)	—[a]
	5.13	3.70[b]	0.82(1)
0.030	4.22	0.83(1)	—[a]
	5.13	5.55[b]	0.53(1)
0.040	4.22	1.10(1)	—[a]
	5.13	7.40[b]	0.42(2)
0.050	4.22	1.29(1)	—[a]
	5.13	9.25[b]	0.57(2)

[a] Rate data fitted by only one exponential, see text. [b] Fixed value of rate constant.

Table 3 Observed rate constants, k_{ox} and k_2, for oxidation of cobalt(II) by peroxomonosulfate in the presence of molybdate: pH dependence ($[Co^{2+}] = 0.0025$ mol dm^{-3}, $[MoO_4^{2-}]_T = 0.0625$ mol dm^{-3}, $[HSO_5^-] = 0.030$ mol dm^{-3}, $I = 1.00$ mol dm^{-3}, 25.0 °C)

pH	k_{ox}/s^{-1}	k_2/s^{-1}	$[MoO_4^{2-}]_{calc}$*/ mol dm^{-3}
4.05	0.98(1)	0.29(1)	0.000 542
4.35	1.40(1)	0.29(1)	0.001 20
4.68	2.37(1)	0.35(1)	0.002 85
4.98	3.55(2)	0.48(1)	0.006 23
5.29	5.69(2)	0.53(1)	0.013 8
5.49	8.22(8)	0.53(1)	0.022 7

* Calculated from data in refs. 23 and 24.

Table 4 Observed rate constants, k_{ox} and k_2, for oxidation of cobalt(II) by peroxomonosulfate in the presence of molybdate: molybdate dependence ($[Co^{2+}] = 0.0015$ mol dm^{-3}, $[HSO_5^-] = 0.0180$ mol dm^{-3}, pH 5.20 ± 0.01, $I = 1.60$ mol dm^{-3}, 25.0 °C)

$[MoO_4^{2-}]_T$/ mol dm^{-3}	k_{ox}/s^{-1}	k_2/s^{-1}	$[MoO_4^{2-}]_{calc}$*/ mol dm^{-3}
0.0750	4.28(1)	0.36(1)	0.0116
0.1125	3.93(1)	0.32(1)	0.0121
0.1500	3.41(1)	0.29(1)	0.0123
0.2250	2.83(1)	0.19(1)	0.0134
0.3000	2.18(1)	0.12(1)	0.0144

* Calculated from data in refs. 23 and 24.

total added $[MoO_4]^{2-}$ were examined. The variation with pH (Fig. 2) is non-linear, a plot of log k_{ox} *vs.* log $[H^+]$ being linear [slope = −0.64(2), $R^2 = 0.998$], while at pH 5.20 k_{ox} shows what appears to be an inverse linear relationship with total added molybdate, $[MoO_4^{2-}]_T$ (Fig. 3). The behaviour in both cases is actually a result of changes in the speciation of molybdate, *i.e.* $[MoO_4]^{2-}$, $[HMoO_4]^-$, H_2MoO_4, $[Mo_7O_{24}]^{6-}$ and $[HMo_7O_{24}]^{5-}$, with both pH and concentration. There have been a considerable number of studies on the speciation of molybdate with both pH and concentration.[25–27] The present kinetic study was carried out at $I = 1.00$ (pH dependence) or 1.60 mol dm^{-3} ($[MoO_4^{2-}]$ dependence) in acetic acid–NaOH buffer solution. While no speciation studies have actually been carried out in this medium, we have found that the formation constants reported by Ozeki *et al.*[23,24] in 3 mol dm^{-3} $NaClO_4$ to be satisfactory for our purposes.

Table 5 Observed rate constants, k_{ox} and k_2, for oxidation of cobalt(II) by peroxomonosulfate in the presence of molybdate: temperature dependence ($[Co^{2+}] = 0.0025$ mol dm^{-3}, $[MoO_4^{2-}]_T = 0.0625$ mol dm^{-3}, $[HSO_5^-] = 0.030$ mol dm^{-3}, pH 5.10 ± 0.01, $I = 1.00$ mol dm^{-3})

T/°C	k_{ox}/s^{-1}	k_2/s^{-1}
15.0	1.59(1)	0.40*
20.0	2.91(2)	0.46*
25.0	5.55(3)	0.52(5)
30.0	8.64(4)	0.58(5)
35.0	13.20(10)	0.65(10)

* Not well defined under the experimental conditions and fixed at these values.

Table 6 Observed rate constants for the ligand-replacement step and associated product distribution; $[Co^{2+}] = 0.010$ mol dm^{-3}, $[MoO_4^{2-}]_T = 0.250$ mol dm^{-3}, $[HSO_5^-] = 0.010$ mol dm^{-3}, $I = 1.40$ mol dm^{-3}, 25.0 °C

pH	$10^4 k_3/s^{-1}$	% Dimer	% Monomer
4.08	2.43(4)	82.5	17.5
4.36	3.79(5)	89.5	10.5
4.71	4.57(5)	90.3	9.7
4.98	5.06(5)	91.3	8.7
5.28	5.36(6)	96.6	3.4

For the molybdate-dependence study, over the range of concentrations examined (0.075–0.300 mol dm^{-3}), the major species in solution are $[Mo_7O_{24}]^{6-}$ and $[MoO_4]^{2-}$ with considerably lower concentrations of $[HMoO_4]^-$, H_2MoO_4 and $[HMo_7O_{24}]^{5-}$. Now, assuming that the differences in molybdate speciation under the experimental conditions of this study and those employed in estimation of the formation constants are not great, as found previously in the Mn^{2+}–$[MoO_4]^{2-}$–HOCl study,[3] then the actual $[MoO_4]^{2-}$ concentrations in solution, *i.e.* $[MoO_4^{2-}]_{calc}$, for various amounts of total added molybdate, at constant pH, may be used to establish the actual molybdate dependence. A plot of log k_{ox} against log $[MoO_4^{2-}]_{calc}$ was linear ($R^2 = 0.9825$) with a slope of −3.07(3), which indicates an inverse third-order dependence on $[MoO_4^{2-}]_{calc}$.

The inverse third-order dependence on $[MoO_4^{2-}]$ can now be included in the rate expression to give equation (2) where k''_{ox}

$$+d[Co^{III}]/dt = k''_{ox}[Co^{2+}][HSO_5^-]/[MoO_4^{2-}]^3 \quad (2)$$

is $1.68(2) \times 10^{-8}$ mol^2 dm^6 s^{-1} at 25 °C based on the actual $[MoO_4]^{2-}$ concentration present in solution at pH 5.20 as calculated from the reported formation constants.

With the dependence of k_{ox} on $[MoO_4^{2-}]$ now established, it is possible to investigate the actual dependence of $[H^+]$ on the trend in k_{ox} with pH by removing the $[MoO_4^{2-}]$ dependence at each pH value. A plot of log $k_{ox}[MoO_4^{2-}]^3$, using the appropriate $[MoO_4^{2-}]_{calc}$ values, against log $[H^+]$ was linear [slope $-4.02(4)$ ($R^2 = 0.9999$)] indicating an inverse fourth-order dependence on $[H^+]$. Thus the rate expression may be further expanded to include this dependence, as in equation (3)

$$+d[Co^{III}]/dt = k'''_{ox}[Co^{2+}][HSO_5^-]/[H^+]^4[MoO_4^{2-}]^3 \quad (3)$$

where $k'''_{ox} = 3.38(2) \times 10^{-25}$ mol^6 dm^{-18} s^{-1} at 25 °C. This value is an average over each of the pH values (4.05–5.49) examined. An alternative form of this rate expression would involve combination of the dependences on $[H^+]$ and $[MoO_4^{2-}]$ through the protonation reaction $H^+ + [MoO_4]^{2-} \longrightarrow [HMoO_4]^-$, for which log $\beta = 3.772$.[24] This in turn leads to a rate expression of the form (4) where $k_{OX} = 7.05(4) \times 10^{-14}$ mol^3 dm^{-9} s^{-1} at 25 °C.

$$+d[Co^{III}]/dt = k_{ox}[Co^{2+}][HSO_5^-]/[H^+][HMoO_4^-]^3 \quad (4)$$

The temperature dependence of the first oxidation step was studied at 15.0–35.0 °C. The data (at pH 5.10) are given in Table 5. An Arrhenius plot of ln k_{OX} against $1/T$ produced a linear relationship ($R^2 = 0.994$) and an Arrhenius activation energy, E_a, of 78.7 kJ mol^{-1}. The linear nature of the plot suggests that there is negligible change in the actual $[MoO_4^{2-}]$ in solution resulting from any change in polymerization over the temperature range studied. In the previous study on the formation of $[MnMo_9O_{32}]^{6-}$ by the oxidation of Mn^{2+}(aq) by HOCl in the presence of molybdate[3] a change in polymerization with temperature was proposed as the cause of the variation in slope of the Arrhenius plot with temperature. However, the temperature range examined was 4.8–20.0 °C rather than 15.0–35.0 °C in the present study, and it may be that increased polymerization occurs only to a significant extent at lower temperatures (*i.e.* less than *ca.* 10–15 °C). The data in Table 5 may also be used to estimate the enthalpy and entropy of activation for this step, and give $\Delta H^{\ddagger} = 76.2$ kJ mol^{-1} and $\Delta S^{\ddagger} = 24.2$ J K^{-1} mol^{-1}. Since solvation effects should dominate in this reaction between ionic species, it is not reasonable to infer much regarding the mechanism from the activation entropy. However, the small positive activation entropy suggests that solvent rearrangement and change in electrostriction in forming the activated state are modest.

Step 2, the ligand breakdown. An examination of the variation of k_2 with $[HSO_5^-]$ at pH 5.13 (with k_{ox} fixed in magnitude for each $[HSO_5^-]$) shows that there is no dependence over the range of HSO_5^- concentrations studied, although even here the error in k_2 is likely to be greater than quoted. Even at this pH, at lower $[HSO_5^-]$, k_2 was not well defined because of the similarity in magnitude of k_{ox} and k_2 and it is only at high $[HSO_5^-]$ where k_{ox} is much greater than k_2 that the latter is sufficiently well defined to indicate that no dependence exists. In contrast, the pH and $[MoO_4^{2-}]$ dependences provide relatively good values for k_2 under the conditions chosen, and indicate that k_2 is independent of both $[H^+]$ and the actual $[MoO_4^{2-}]$ in solution. The variation in k_2 (0.29–0.53 s^{-1}) is considered to be a result of data fitting rather than a true variation with pH. A potential dependence on cobalt concentration was also investigated, which would make this step second order in $[Co^{3+}]$ (allowing it to be attributed to a dimerization step), but was found not to exist. Using initial cobalt(II) concentrations of 0.0025 and 0.0050 mol dm^{-3}, with $[MoO_4^{2-}]_T = 0.050$ mol dm^{-3}, $[HSO_5^-] = 0.050$ mol dm^{-3}, pH 5.67 ± 0.01, $I = 1.00$ mol dm^{-3} and $T = 25.0$ °C, the values of the rate constants k_{ox} and k_2 were 19.98(10) and 0.40(1) and 18.10(10) and 0.38(1) s^{-1}, respectively. The slight variations between the results at the two cobalt concentrations are again attributed to data fitting.

Step 3, the ligand replacement. The third kinetically observed step was considerably slower than either of the above steps, taking some 3 h to go to completion at 25 °C. The reaction was first order, and showed no real dependence on $[MoO_4^{2-}]$, with the slight variation of k_3 being attributable to the change in ionic make up of the solutions. There was, however, a significant dependence on pH (Table 6), with k_3 apparently decreasing as the pH decreased. A plot of log k_3 *vs.* log $[H^+]$ was non-linear, indicating no simple relationship linking these properties.

Mechanistic considerations

For the rate law established above for the first (oxidation) step a possible reaction mechanism can now be proposed. The rate expression suggests that prior to oxidation three protonated molybdate units are lost from a cobalt(II) heteropolymolybdate followed by the loss of a single hydrogen ion, which then allows the HSO_5^- to enter the primary co-ordination sphere of the Co^{II} and effect a one-electron oxidation of Co^{II} to Co^{III}. The likely cobalt(II) heteropolymolybdate species is that described above, *i.e.* $[H_6CoMo_6O_{24}]^{4-}$, which may be crystallized from solution in the pH range that pertains to this study.

We considered the equilibria (5)–(8) followed by the rate-

$$[H_6Co^{II}Mo_6O_{24}]^{4-} \underset{k_{-1}}{\overset{k_1}{\rightleftharpoons}} [H_5Co^{II}Mo_5O_{20}]^{3-} + HMoO_4^- \quad (5)$$

$$[H_5Co^{II}Mo_5O_{20}]^{3-} \underset{k_{-2}}{\overset{k_2}{\rightleftharpoons}} [H_4Co^{II}Mo_4O_{16}]^{2-} + HMoO_4^- \quad (6)$$

$$[H_4Co^{II}Mo_4O_{16}]^{2-} \underset{k_{-3}}{\overset{k_3}{\rightleftharpoons}} [H_3Co^{II}Mo_3O_{12}]^- + HMoO_4^- \quad (7)$$

$$[H_3Co^{II}Mo_3O_{12}]^- \underset{k_{-4}}{\overset{k_4}{\rightleftharpoons}} [H_2Co^{II}Mo_3O_{12}]^{2-} + H^+ \quad (8)$$

determining step (9) where the oxidized cobalt(III) product is a

$$[H_2Co^{II}Mo_3O_{12}]^{2-} + HSO_5^- \xrightarrow{k_5} [H_2Co^{III}Mo_3O_{12}(HSO_5)]^{3-} \text{ (radical)} \quad (9)$$

radical species, with the electron probably localized on an 'HSO_5^{2-}' (radical) ligand, formed following reduction of the HSO_5^- oxidant. It should be noted that the above equations have been written without the express involvement of the solvent as this cannot be established, but which is certainly going to involve rapid addition/loss to Co^{II}, presumably maintaining six-co-ordination.

Now, from equilibria (5)–(8) expression (10) can be derived.

$$[H_2CoMo_3O_{12}^{2-}] = k_1k_2k_3k_4[H_6CoMo_6O_{24}^{4-}]/k_{-1}k_{-2}k_{-3}k_{-4}[H^+][HMoO_4^-]^3 \quad (10)$$

As the kinetic equation for the rate-determining step is (11), combining equations (10) and (11) gives expression (12) for the

rate-determining step, which may be written as (13) where $k = k_1k_2k_3k_4k_5/k_{-1}k_{-2}k_{-3}k_{-4}$. This is equivalent to equation (4), with $k = k_{OX}$, assuming that the pre-equilibria (5)–(8) are fast compared to k_5, the rate-determining step [equation (9)].

$$+d[Co^{III}]/dt = k_5[H_2Co^{II}Mo_3O_{12}^{2-}][HSO_5^-] \quad (11)$$

$$+d[Co^{III}]/dt = k_1k_2k_3k_4k_5[H_6CoMo_6O_{24}^{4-}][HSO_5^-]/k_{-1}k_{-2}k_{-3}k_{-4}[H^+][HMoO_4^-]^3 \quad (12)$$

$$+d[Co^{III}]/dt = k[H_6Co^{II}Mo_6O_{24}^{4-}][HSO_5^-][H^+][HMoO_4^-]^3 \quad (13)$$

The rate law and mechanism are consistent with a series of fast equilibria involving loss (and consequently addition) of $[HMoO_4]^-$ (or H^+ and MoO_4^{2-}, it is impossible to say which) around Co^{II} in solution, probably involving the Anderson-based $[H_6Co^{II}Mo_6O_{24}]^{4-}$ structure and fragments derived from this anion. Of course, these equilibria occur naturally in an acidic cobalt(II)–molybdate solution, and are not dependent on the presence of the HSO_5^- oxidant. The substrate actually oxidized can reasonably be assumed to be solvated $[H_2Co^{II}Mo_3O_{12}]^{2-}$, which involves loss of three $[HMoO_4]^-$ ions and an H^+ from $[H_6Co^{II}Mo_6O_{24}]^{4-}$. The latter loss of an H^+ can be rationalized by noting that, following removal of three $[HMoO_4]^-$ ions, of the three remaining protons only two remain in environments identical to that prior to the fragmentation, while the third is now bound to an oxygen that is exposed and only two-co-ordinate to Co^{II}. This presumably leads to a lower pK_a for this hydrogen, and its subsequent loss. The putative solvated $[H_2Co^{II}Mo_3O_{12}]^{2-}$ ion could be considered as having the Co^{II} in an octahedral environment of the oxygen atoms of two solvent water molecules and a condensed polymolybdate ligand derived from three $[MoO_4]^{2-}$ ions, which provide the other four oxygen-donor atoms. Exchange of the water molecules is presumably very fast, allowing facile co-ordination of a unidentate or chelating HSO_5^- ion, subsequently leading to a one-electron oxidation of Co^{II} to Co^{III}. Electron transfer is thus facilitated by co-ordination, and is effectively intramolecular. The oxidation step is slower than the reversible loss of $[HMoO_4]^-$ and H^+ from the labile precursor, and hence it is the rate-determining step. The resulting cobalt(III) species has a partially built polymolybdate environment and presumably a co-ordinated radical 'HSO_5^{2-}' ligand bound in its primary co-ordination shell, the extra electron from the oxidation now being localized on the (reduced) 'HSO_5^{2-}' ligand. We note in passing that the mechanism of electron transfer in the present case is quite different from the oxidation of the Keggin-type $[Co^{II}W_{12}O_{40}]^{6-}$ species by HSO_5^- in the presence of added tungstate over the same pH range, which gives $[Co^{III}W_{12}O_{40}]^{5-}$.[28] In the latter example there is no dependence of the rate of oxidation on the oxidant concentration, which we interpret as an example of the slow, rate-determining breakdown of the polytungstate Keggin unit surrounding the Co^{II}, and reflects the relative ease of dissociation of $[WO_4]^{2-}$ *versus* $[MoO_4]^{2-}$ from polyoxometalate structures under acidic conditions.

The second kinetically observable step has no dependences on $[Co^{III}]$, pH, $[MoO_4^{2-}]$ or $[HSO_5^-]$ and the rate constant is 0.41(5) s^{-1} (mean and standard error over all data) at 25 °C. This precludes, for example, ligand substitution around Co^{III} and can therefore be associated with a reaction involving the ligands. It likely involves breakdown of the radical 'HSO_5^{2-}' ligand to give an SO_4^{2-} ligand and an OH• radical. All attempts to observe an ESR signal in solution at 21 °C immediately after the oxidation step were unsuccessful (within 40–60 s following mixing of the reagents), which supports the fast loss of the radical nature of the immediate oxidation product. As the lifetime of an OH• radical in aqueous solution is short (*e.g.* the bimolecular rate constants for reaction of OH• with solutes typically range from 10^7 to 10^9 dm^3 mol^{-1} s^{-1} at 25 °C),[29] the formation of this species offers a plausible mechanism for radical loss. Moreover, as discussed below, the absorbance maximum at 622 nm of the product of this step is consistent with the formation of a cobalt(III) sulfato species, which also supports formation of an SO_4^{2-} ligand bound to Co^{III} by loss of an OH• radical in this step. Following the ligand breakdown step, dimerization of two partially formed fragments each derived from the Anderson structure (and containing a co-ordinated SO_4^{2-}) is assumed to occur, but this is not kinetically observable.

The intermediate cobalt(III) species formed after the above reactions has an absorbance maximum for the $^1A_{1g} \longrightarrow {}^1T_{1g}$ (O_h symmetry) electronic transition (622 nm) at lower energies than those of either $[H_6CoMo_6O_{24}]^{3-}$ or $[H_4Co_2Mo_{10}O_{38}]^{6-}$ (both 599 nm), and also a much higher molar absorption coefficient than either of these species. The latter suggests low-symmetry (distorted) environments for both cobalt(III) centres in the immediate product of the dimerization. The observed value for the $^1A_{1g} \longrightarrow {}^1T_{1g}$ transition is shifted significantly to lower energies than those found for $[Co(C_2O_4)_3]^{3-}$ (599 nm)[30] and $[Co(H_2O)_6]^{3+}$ [606 nm for $CsCo(SO_4)_2{\cdot}12H_2O$, a cubic β-alum structure][30] and in anhydrous $Co(NO_3)_3$ (which has three bidentate NO_3^- ligands, 613 nm in CCl_4).[31,32] The lower-energy transition is therefore consistent with the presence of a weakly bound oxygen-donor ligand species, most likely a SO_4^{2-} attached to Co^{III} as part of an octahedral (*i.e.* six-co-ordinate) oxygen-atom environment. The molar absorption coefficient of this species then decays slowly over approximately 3 h at 25 °C indicating conversion into a product(s) with an absorption coefficient between that of the monomer and dimer, and a pH-dependent product distribution. The data for the product distribution over the range pH 4.08–5.28 are given in Table 6. It is proposed that this decay step is most likely attributable to the loss of the weakly bound SO_4^{2-} ligands, one from each Co^{III} in the dimeric structure. This must be followed by the rapid addition of $[MoO_4]^{2-}$ which results in the condensed polymolybdate environment surrounding the two cobalt(III) ions in the completed dimeric structure of $[H_4Co_2Mo_{10}O_{38}]^{6-}$. A pH dependence was observed with a decrease in rate as the acidity increased for this kinetically observable step. The observed pH dependence is most likely due to the fact that the dimer species is known to be decomposed by acid. Indeed, acid solutions of the anion are known to produce $[H_6CoMo_6O_{24}]^{3-}$ on standing for several hours and, although solutions of the free acid can be obtained, they also decompose on standing.[5] As the decomposition of $[H_4Co_2Mo_{10}O_{38}]^{6-}$ by acid to give $[H_6CoMo_6O_{24}]^{3-}$ occurs over the same time frame as that of the final kinetically observable step which gives rise to formation of the dimer, it is concluded that the trend to lower values of the observed rate constant with pH really represents a composite of the formation and some concomitant decomposition of $[H_4Co_2Mo_{10}O_{38}]^{6-}$ during formation of the latter. Thus a value for k_3 of *ca.* 5.5×10^{-4} s^{-1} at 25 °C (obtained by extrapolation to pH 5.5) represents the true rate constant, assuming no decomposition of $[H_4Co_2Mo_{10}O_{38}]^{6-}$, for the final kinetically observable step involving loss of co-ordinated SO_4^{2-} from a dimeric $Co^{III}{}_2$ polymolybdate unit.

Finally, as in the previously studied Mn^{2+}–$[MoO_4]^{2-}$–HOCl system,[3] the kinetics and derived mechanism established above again indicate the involvement of $[MoO_4]^{2-}$ and/or $[HMoO_4]^-$ in the assembly (and disassembly) of a condensed polymolybdate cage surrounding the heteroatom in a heteropolymolybdate, in this case $[H_4Co_2Mo_{10}O_{38}]^{6-}$. Moreover, this study is the first to provide actual kinetic and mechanistic evidence for the formation of a large polyoxometalate anion containing two heteroatoms, and shows that two partially

built heteropolyoxometalate cages can join (dimerize) to produce a larger species.

Acknowledgements

We thank Mr. D. C. Craig of the School of Chemistry, The University of New South Wales, for collecting the crystal data, the absorption correction and for data reduction, Ms. C. Allen, The University of Newcastle, for help in the structural solution and preparation of the ORTEP diagram, and Ms. J. Irwin for help in the ESR study. The Universities of Sydney and New South Wales are also acknowledged for providing access to the Bruker ESP300 spectrometer. We also acknowledge receipt of an Australian Postgraduate Award (to A. L. N.).

References

1 S. J. Dunne, R. C. Burns, T. W. Hambley and G. A. Lawrance, *Aust. J. Chem.*, 1992, **45**, 685.
2 S. J. Dunne, R. C. Burns and G. A. Lawrance, *Aust. J. Chem.*, 1992, **45**, 1943.
3 S. J. Angus-Dunne, J. A. Irwin, R. C. Burns, G. A. Lawrance and D. C. Craig, *J. Chem. Soc., Dalton Trans.*, 1993, 2717.
4 G. A. Tsigdinos, Ph.D. Thesis, Boston University, 1961.
5 L. C. W. Baker, B. Loev and T. P. McCutcheon, *J. Am. Chem. Soc.*, 1956, **72**, 2374.
6 K. Nomiya, M. Wada, H. Murasaki and M. Miwa, *Polyhedron*, 1987, **6**, 1343.
7 A. La Ginestra, F. Gianetta and P. Fiorucci, *Gazz. Chim. Ital.*, 1968, **98**, 1197.
8 H. T. Evans, jun., and J. S. Showell, *J. Am. Chem. Soc.*, 1969, **91**, 6881.
9 M. Maeder and A. Zuberbühler, *Anal. Chem.*, 1990, **62**, 2220.
10 A. I. Vogel, *A Text-book of Quantitative Inorganic Analysis including Elementary Instrumental Analysis*, 3rd edn., Longmans, London, 1961, p. 298, Procedure B.
11 J. de Meulenaer and H. Tompa, *Acta Crystallogr.*, 1965, **19**, 1014.
12 G. M. Sheldrick, *Acta Crystallogr., Sect. A*, 1990, **46**, 467.
13 G. M. Sheldrick, Program for Crystal Structure Refinement, University of Göttingen, 1993.
14 H. T. Evans, jun., B. M. Gatehouse and P. Leverett, *J. Chem. Soc., Dalton Trans.*, 1975, 505.
15 W. J. Seimons and D. H. Templeton, *Acta Crystallogr.*, 1954, **7**, 194.
16 C. K. Johnson, ORTEP II, A Thermal Ellipsoid Plotting Program, Oak Ridge National Laboratory, Oak Ridge, TN, 1976.
17 A. Perloff, *Inorg. Chem.*, 1970, **9**, 2228.
18 F. A. Cotton, L. M. Daniels, C. A. Murillo and J. F. Quesada, *Inorg. Chem.*, 1993, **32**, 4861.
19 E. F. K. McCandlish, T. K. Michael, J. A. Neal, E. C. Lingafelter and N. J. Rose, *Inorg. Chem.*, 1978, **17**, 1383.
20 F. A. Cotton and R. Eiss, *J. Am. Chem. Soc.*, 1968, **90**, 38 and refs. therein.
21 N. C. Tombs and H. P. Rooksby, *Nature (London)*, 1950, **165**, 442.
22 K. Nomiya, T. Takahashi, T. Shirai and M. Miwa, *Polyhedron*, 1987, **6**, 213.
23 T. Ozeki, H. Kihara and S. Hikime, *Anal. Chem.*, 1987, **59**, 945.
24 T. Ozeki, H. Kihara and S. Ikeda, *Anal. Chem.*, 1988, **60**, 2055.
25 M. T. Pope, *Heteropoly and Isopoly Oxometalates*, Springer, Berlin, 1983, ch. 3, section E.
26 L. Pettersson, *Polyoxometalates: From Platonic Solids to Anti-Retroviral Activity*, eds. M. T. Pope and A. Müller, Kluwer, Dordrecht, 1994, p. 27.
27 P. L. Brown, M. E. Shying and R. N. Sylva, *J. Chem. Soc., Dalton Trans.*, 1987, 2149.
28 A. L. Nolan, R. C. Burns and G. A. Lawrance, in preparation.
29 E. Hayon, *Radiation Chemistry of Aqueous Systems*, ed. G. Stein, Weizmann Science Press-Interscience, New York, 1968, p. 157.
30 D. A. Johnson and A. G. Sharpe, *J. Chem. Soc. A*, 1966, 798.
31 R. J. Fereday, N. Logan and D. Sutton, *Chem. Commun.*, 1968, 271.
32 J. Hilton and S. C. Wallwork, *Chem. Commun.*, 1968, 871.

Received 4*th December* 1995; *Paper* 5/07852K